

## Numerical Modeling of AGN Jets: Formation of Magnetically Dominated Lobes and Stability Properties of Current-carrying Jets

M. Nakamura, H. Li, S. Diehl, and S. Li

*Theoretical Division, Los Alamos National Laboratory, Los Alamos, NM 87545, U.S.A*

**Abstract.** We argue the behavior of Poynting flux-dominated outflows from AGN in the galactic cluster systems by performing three-dimensional MHD simulations within the framework of the "magnetic tower" model. Of particular interests are the structure of MHD waves, the cylindrical radial force balance, the (de)collimation, and the stability properties of magnetic tower jets. Transition between the jet/lobe and the formation of wiggling jet by growing current-driven instability are discussed.

### 1. Introduction

Magnetohydrodynamic (MHD) mechanisms are often invoked to explain the launching, acceleration and collimation of jets from Young Stellar Objects, X-ray binaries, Active Galactic Nuclei (AGNs), Microquasars, and Quasars (see, *e.g.*, Meier et al. 2001, and references therein). Strongly magnetized jets, particularly those with a strong toroidal field encircling the collimated flow, are often referred to as "current-carrying" or "Poynting flux-dominated" (PFD) jets. A large current flowing parallel to the jet flow is responsible for generating a strong, tightly wound helical magnetic field. The global picture of a current-carrying jet with a closed current system linking the magnetosphere of the central engine and the hot spots was introduced by Benford (1978, 2006) and applied to AGN double radio sources. This closed current system includes a pair of current circuits, each containing both a forward electric current path (the jet flow itself, with its toroidal magnetic field, toward the lobe), and a return electric current path (along some path back to the AGN core).

Theory of magnetically driven outflows in the electromagnetic regime has been proposed by Blandford (1976) and Lovelace (1976) and subsequently applied to rotating black holes (Blandford & Znajek 1977) and to magnetized accretion disks (Blandford & Payne 1982). An underlying large-scale poloidal field for producing the magnetically driven jets is almost universally assumed in many theoretical/numerical models. However, the origin and existence of such a galactic magnetic field are still poorly understood. In contrast with the large-scale field models, Lynden-Bell (Lynden-Bell 1996) examined the "magnetic tower"; expansion of the local force-free magnetic loops anchored to the star and the accretion disk by using the semi-analytic approach. Global magnetostatic solutions of magnetic towers with external thermal pressure were also computed by Li et al. (2001) using the Grad-Shafranov equation in axisymme-

try. Full three-dimensional MHD numerical simulations of magnetic towers have been performed by Kato et al. (2004).

Recent X-ray and radio observations have revealed the dynamical interaction between the outbursts driven by AGN and the background IGM/ICM, such as X-ray "cavities" with corresponding radio "bubbles" (Fabian et al. 2000; Croston et al. 2003; Kraft et al. 2006; Wise et al. 2007; Gitti et al. 2007). The cavities are believed to be filled with very low density relativistic plasma, inflated from the electromagnetic jets that are being powered by AGNs. This paper describes nonlinear dynamics of propagating magnetic tower jets in galaxy cluster scales ( $>$  tens of kpc) based on three-dimensional MHD simulations to argue the jet/lobe transition (Nakamura et al. 2006) and the stability properties (Nakamura et al. 2007).

## 2. Numerical Setup

We solve the nonlinear system of time-dependent ideal MHD equations numerically in a 3-D Cartesian coordinate system  $(x, y, z)$ . The basic numerical treatments are introduced in Li et al. (2006); Nakamura et al. (2006, 2007). We assume an initial hydrostatic equilibrium in the gravitationally stratified medium, adopting an iso-thermal King model (King 1962) to model the magnetic towers from AGNs in galaxy cluster systems. AGN accretion disk can not be resolved in our computational domain, and thus the magnetic flux and the mass are steadily injected in a central small volume during a certain time period. Since the injected magnetic fields are not force-free, they will evolve as a "magnetic tower" and interact with the ambient medium. In the present paper, we present two different runs: one is called the "unperturbed case" in the following discussion, which is a run without any initial perturbation to the background initial profiles (Nakamura et al. 2006). The other is called the "perturbed case", where a finite amplitude perturbation (a few percent of the background sound speed) is given to the velocities of the background gas (Nakamura et al. 2007).

The total computational domain is taken to be  $|x|, |y|, |z| \leq 16$  corresponding to a  $(160 \text{ kpc} : -80 \text{ to } 80 \text{ kpc})^3$  box. The numerical grids are  $240^3$  in the unperturbed case and  $320^3$  in the perturbed case. Normalizing factors are a length  $R_0 = 5 \text{ kpc}$ , a sound speed  $C_{s0} = 4.6 \times 10^7 \text{ cm s}^{-1}$ , a time  $t_0 = 1.0 \times 10^7 \text{ yr}$ , a density  $\rho_0 = 5.0 \times 10^{-27} \text{ g cm}^{-3}$ . The corresponding unit pressure  $p_0$  as  $\rho_0 C_{s0}^2 = 1.4 \times 10^{-11} \text{ dyn cm}^{-2}$ , and the unit magnetic field  $B_0$  as  $\sqrt{4\pi\rho_0 C_{s0}^2} = 17.1 \mu\text{G}$ . The initial sound speed in the simulation is constant,  $C_s = \gamma^{1/2} \approx 1.29$ , throughout the computational domain, which give a sound crossing time  $\tau_s \approx 0.78$ , corresponding to a typical time scale  $R_0/C_{s0} \approx 10.0 \text{ Myr}$ . Therefore,  $t = 1$  is equivalent to the unit time scale 12.8 Myr. In the King model we use here, we adopt the cluster core radius  $R_c$  to be 4.0 (i.e., 20 kpc) and the slope  $\kappa$  to be 1.0 in the unperturbed case and 0.75 in the perturbed case. Magnetic fluxes and mass are continuously injected into a central volume of the computational domain for  $t_{\text{inj}} = 3.1$ , after which the injection is turned off. A magnetic energy injection rate is  $\sim 10^{43} \text{ ergs s}^{-1}$ , a mass injection rate is  $\sim 0.046 M_\odot/\text{yr}$ , and an injection time is  $\sim 40 \text{ Myr}$ .

### 3. Results

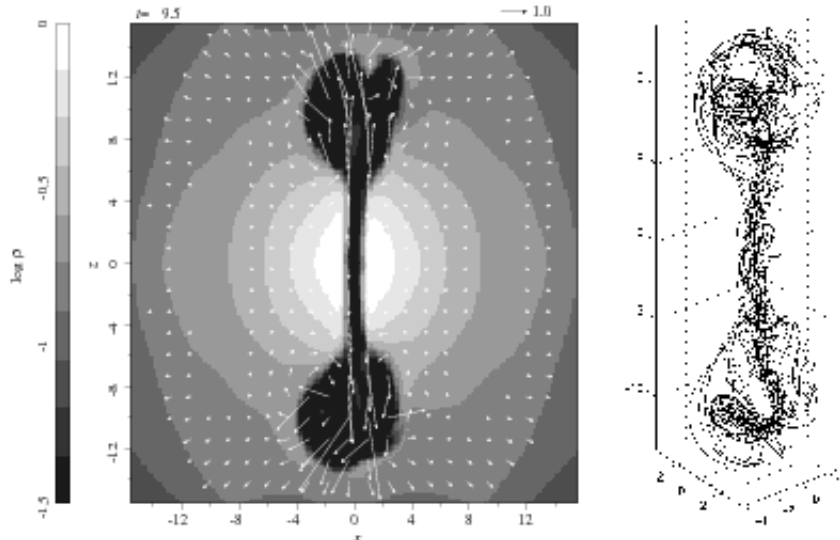


Figure 1. Distribution of density in the  $x-z$  plane along with the poloidal velocity (*left*) and three-dimensional view of selected magnetic field lines (*right*) for the perturbed case.

During the dynamical evolution of magnetic tower jet, the narrow “jet body” and the expanded “lobe” are formed as shown in Fig. 1 (*left*). The 3D view of magnetic field lines as illustrated in Fig. 1 (*right*) indicates that the magnetic tower jet has a well-ordered helical field configuration showing that a tightly wound central helix goes up along the central axis and a loosely wound helix comes back at the outer edge of the magnetic tower. The profiles of underlying external gas plays an important role in the transition of jet/lobe. The jet body is confined jointly by the external pressure and the gravity inside  $R_c$ , while it expands radially beyond  $R_c$  to form the lobe in a steeply decreasing ambient pressure.

The jet axial current and the ambient gas pressure can determine the radius of the magnetically dominated lobes (Nakamura et al. 2006), that is, the internal gas pressure plays a minor role in the lobes which are typically seen in FR I radio galaxies (Croston et al. 2003). Our numerical result shows the magnetically dominated lobes expand subsonically which can be seen in some observations (Kraft et al. 2006). A preceding hydrodynamic shock wave beyond the tower, which may be identified as an AGN-driven shock in recent X-ray observations (Forman et al. 2005; Fabian et al. 2006).

The outer edge of the magnetic tower may be identified as a tangential discontinuity without the normal field component. The interior of tower (lobe) is separated from the non-magnetized external gas via this discontinuity. Figure 2 shows the distributions of forces (*left*) and the magnetic field components (*right*) along the radial directions. At the tower edge, the outwardly directed magnetic

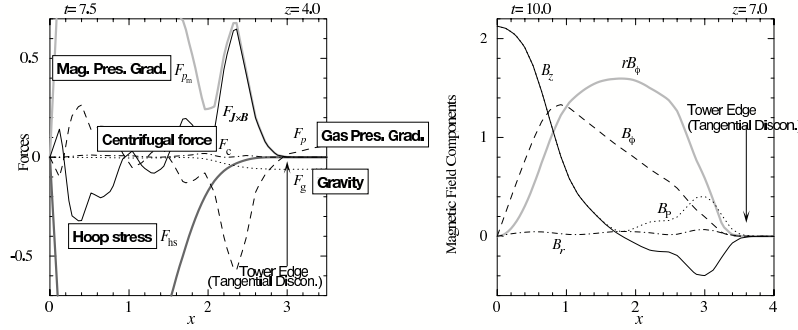


Figure 2. Radial profiles of the forces (*left*) and the magnetic field components (*right*) along the  $x$ -axis for the unperturbed case. The position of the magnetic tower edge is shown.

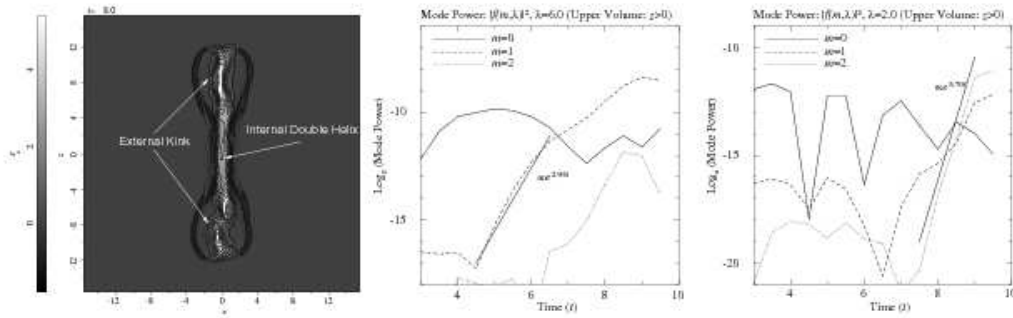


Figure 3. Distribution of axial current density in the  $x - z$  (*left*) for the perturbed case. Time variation of the azimuthal Fourier power of the current density with the axial ( $z$ ) wavelengths  $\lambda = 6.0$  (*middle*) and  $\lambda = 2.0$  (*right*).

pressure gradient force is roughly balanced with the inwardly directed thermal pressure gradient force. On the other hand, at the core part of jet body, the quasi-force free equilibrium is achieved. In the context of magnetically controlled fusion systems, the helical field in the magnetic tower can be regarded as the reversed field pinch (RFP) profile.

The current-carrying magnetic tower jet, which possesses a highly wound helical field, is subject to the current-driven instability (CDI). Although the destabilizing criteria will be modified by the ambient gas and the RFP configuration of the tower, we find that the propagating magnetic tower jets can develop the non-axisymmetric CDI modes. Both the internal elliptical ( $m = 2$ ) mode (Fig. 3 *right*) like the “double helix” and the external kink ( $m = 1$ ) mode (Fig. 3 *middle*) grow to produce the wiggles at the different parts (Fig. 3 *left*) (Nakamura et al. 2007). This morphological feature (the jet is suddenly disrupted at the lobe region with visible [external] wiggles) can be observed in Hercules A (Gizani & Leahy 2003).

#### 4. Conclusion

By performing 3D MHD simulations, we have investigated the nonlinear dynamics of magnetic tower jets in the galaxy cluster system. Under the gravitationally stratified atmosphere, the magnetic tower jet forms a global current closure system having the reverse field pinch magnetic configuration. The magnetic tower jet is well confined by the external gas pressure to form the collimated “jet body” inside the cluster core radius. The narrow jet expands radially to form the magnetically dominated “lobe” beyond the cluster core radius. Thus, the profiles of underlying external gas play an important role in the transition of jets/lobes.

The current-carrying tower jet, which possesses a highly wound helical magnetic field, is subject to the current-driven instability. In the gravitationally stratified atmosphere, the effect of thermal confinement on the magnetic tower jet will get gradually weaker as it grows. As a result, a separation of current flowing path between the jet axial current and the return current occurs. Therefore, the edge of the jet axial current becomes a free boundary against the external kink mode to produce the visible wiggles as seen in some observations.

**Acknowledgments.** This work was carried out under the auspices of the National Nuclear Security Administration of the U.S. Department of Energy at Los Alamos National Laboratory under Contract No. DE-AC52-06NA25396. It was supported by the Laboratory Directed Research and Development Program at LANL and by IGPP at LANL.

#### References

- Benford, G. 1978, *MNRAS*, 183, 29  
 Benford, G. 2006, *MNRAS*, 369, 77  
 Blandford, R. D. 1976, *MNRAS*, 199, 883  
 Blandford, R. D., & Znajek, R. L. 1977, *MNRAS*, 179, 433  
 Blandford, R. D., & Payne, D. G. 1982, *MNRAS*, 199, 883  
 Croston, J. H., Hardcastle, M. J., Birkinshaw, M., & Worrall, D. M. 2003, *MNRAS*, 346, 1041  
 Fabian, A. et al. 2000, *MNRAS*, 318, L65  
 Fabian, A. et al. 2006, *MNRAS*, 366, 417  
 Forman, W. et al. 2005, *ApJ*, 635, 894  
 Gitti, M., McNamara, B. R., Nulsen, P. E. J., & Wise, M. W. 2007, *ApJ*, 660, 1118  
 Gizani, N. A. B. & Leahy J. P. 2003, *MNRAS*, 342, 399  
 Kato, Y., Mineshige, S., & Shibata, K. 2004, *ApJ*, 605, 307  
 Kraft R. P., Azcona, J., Forman, W. R., Hardcastle M. J., Jones, C., & Murray, S. S. 2006, *ApJ*, 639, 753  
 King, I. 1962, *AJ*, 67, 471  
 Li, H., Lovelace, R. V. E., Finn, J. M., & Colgate, S. A. 2001, *ApJ*, 561, 915  
 Li, H., Lapenta, G., Finn, J. M., Li, S., & Colgate, S. A. 2006, *ApJ*, 643, 92  
 Lovelace, R. V. E. 1976, *Nature*, 262, 649  
 Lynden-Bell, D. 1996, *MNRAS*, 279, 389  
 Meier, D. L., Koide, S., & Uchida, Y. 2001, *Science*, 291, 84  
 Nakamura, M., Li, H., & Li, S. 2006, *ApJ*, 652, 1059  
 Nakamura, M., Li, H., & Li, S. 2007, *ApJ*, 656, 721  
 Wise, M. W., McNamara, B. R., Nulsen, P. E. J., Houck, J. C., & David, L. P. 2007, *ApJ*, 659, 1153